Int. J. Electrochem. Sci., 11 **(2016)** 6229 – 6243, doi: 10.20964/2016.07.10

International Journal of
ELECTROCHEMICAL
SCIENCE
www.electrochemsci.org

Inhibition Effect of Water-Soluble Chitosan N-quaternary Ammonium Salt on Carbon Steel in 0.25 M H_2SO_4 Solution

Xiumei Wang[*], *Qing Wang, Ye Wan, Ying Ma*

School of Materials Science and Engineering, Shenyang Jianzhu University, Shenyang, Liaoning, China 110168
[*]E-mail: xmwang@alum.imr.ac.cn

Received: 4 March 2016 / *Accepted:* 29 April 2016 / *Published:* 4 June 2016

The corrosion inhibition of modified natural product (2-hydroxypropyltrimethyl ammonium chloride chitosan (HACC) for carbon steel in 0.25 M H_2SO_4 solution was studied through four methods including weight loss method, potentiodynamic polarization curves, electrochemical impedance spectroscopy (EIS) and scanning electron microscopy (SEM) techniques. The concentration of HACC and solution temperature affected HACC inhibition efficiency. The weight loss results indicated the high HACC concentration and low temperature lead to good inhibition. HACC was a mixed inhibitor by retarding both anodic and cathodic processes simultaneously. Standard free adsorption energy ΔG^{o}_{ads} was calculated and discussed. The adsorption of HACC obeyed the Langmuir isotherm and was of spontaneous characteristic accompanied by joint physisorption and chemisorption. The corrosion rate of carbon steel was mainly controlled by E_a in 0.25 M H_2SO_4 solution.

Keywords: Carbon steel; EIS; Polarization Curves; Sulfuric Acid; Inhibition Efficiency**1.**

INTRODUCTION

Various metal equipments such as reaction vessels, pipelines (water, gas and oil) and storage tanks are used extensively in many industrial fields. Carbon steel with high tenacity and good moldability is the main material to fabricate these equipments. Among these practical processes, hydrochloric and sulfuric acid solutions are the most common used agents leading to high corrosion rate of carbon steel because of its exposure to aggressive acid media resulting in economic losses and safety accidents, especially acid pickling, chemical cleaning of boilers, oil and gas recovery [1].

This becomes the main obstacle for the use of carbon steel in more fields [2]. Carbon steel in sulfuric acid solution is corroded more heavily than that in hydrochloric acid solution. People found several methods to protect carbon steel from acid corrosion, such as addition of corrosion inhibitor, cathodic protection, coating. A small amount of corrosion inhibitor effectively prevents metal from

corrosion. The addition of corrosion inhibitor has become an effective method for metal against acid corrosion due to its high inhibition performance, simplicity of operation and considerable economic benefit on a world-wide scale [3]. In recent years, it has been reported in considerable details the prevention of organic compounds on carbon steel corrosion in corrosive electrolyte has achieved good effect [4-11]. The obvious characteristic of most organic inhibitors is that their structure contains O, N, P, S, π bond and/or conjugated system which endow organic molecules with the ability to reach metal surface by columbic attractions or transference of unshared electron pair [12-14]. The adsorptive ability of inhibitor on carbon steel surface is the most important factor affecting the inhibition efficiency. Generally, compound with heteroatom may be possible to behave as corrosion inhibitor. A variety of natural products have the potential to be used as corrosion inhibitor due to heteroatom in their structure of active constituents. Natural product chitosan is rich in hydroxyl and amino groups and it is environmental friendly, therefore, chitosan and its derivatives will be a promising inhibitor [15, 16]. In aqueous corrosive solution, the solubility is the prerequisite to determine the effect of corrosion inhibitor. Chitosan and its derivatives have low water-solubility and acid-solubility causing poor adsorption and poor inhibition effect. It is noticed that there is N atom in chitosan structure and N atom is easily modified into N-quaternary ammonium salt with good water-solubility by quaterisation. So the water-soluble chitosan N-quaternary ammonium salt is a promising preference. In this work, the aim is trying to evaluate the inhibition performance of water-soluble N-quaternary ammonium salt of chitosan (2-hydroxypropyltrimethyl ammonium chloride chitosan, HACC) on carbon steel in 0.25 M H_2SO_4 solution employing different methods. Adsorption isotherm is used to illustrate the adsorptive mode of HACC molecule. Influences of HACC concentration and corrosive system temperature on inhibition effect will be made a detailed discussion.

2. EXPERIMENTAL

2.1. Material

For the present work, the carbon steel sample was composed of the below elements: 0.13% C, 0.05% Si, 0.30% Mn, 0.03% P and the remainder Fe. Before experiments, the carbon steels were mechanically made into specimens of 20 mm × 20 mm × 5 mm with a 3 mm hole in diameter for weight loss measurement. The specimens were polished with various grit paper (grade 100–800) gradually, washed with deionized water, put it into beaker containing 20 mL acetone and shook in ultrasonic bath for 10 minutes to remove surface grit and dust, finally dried with compressed air for use. For electrochemical experiments, the carbon steel sample was cut into a cuboid rod with 1 cm length and 1cm^2 exposed surface areas, other surfaces were covered with resin. Before experiments, the exposed surface was polished with grit paper (grade 100–800), rinsed thoroughly with deionized water, degreased with ethanol, put it into beaker containing 20 mL acetone and shook in ultrasonic bath for 10 minutes to remove surface grit and dust, dried with compressed air and kept in desiccators. 0.25 M H_2SO_4 solution was made of AR grade sulfuric acid diluted by deionized water. 2-hydroxypropyltrimethyl ammonium chloride chitosan (HACC, supplied by Nantong Lushen

Bioengineering Co. Ltd. (Jiangsu, China)) was used without purification and it has the following structure (Fig.1).

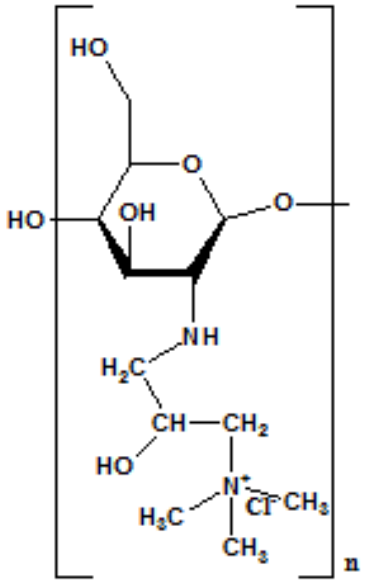

Figure 1. Structure of 2-Hydroxypropyltrimethyl Ammonium Chloride Chitosan (HACC)

2.2. Weight loss measurements

The carbon steel specimens were weighed accurately by scale with ±0.1mg sensitivity, suspended with plastic hooks in triplicate in conical flask containing 250 mL corrosive electrolyte without and with various HACC dosages (10 to 100 mg L^{-1}). The measurements were performed in H_2SO_4 solutions under natural condition. The carbon steel samples were taken out after they were immersed in the corrosive media for 5 h, then flushed with tape water, shook in ultrasonic bath, rinsed thoroughly with deionized water, dried and reweighed accurately. At various temperatures (30-60℃), the experiments were repeated according to the same procedure. The weight loss of each sample was calculated for each corrosive solution. Equation (1) was used to determine the corrosion rate (*CR*).

$$CR = \frac{87.6 \times \Delta W}{\rho A t} \quad (1)$$

where ΔW represents the weight loss of a carbon steel sheet (g), *A* represents the total geometrical area of a sheet (cm^2) exposed to electrolyte, *t* represents the immersion time (h), ρ denotes Fe density (g cm^{-3}). Average *CR* can be calculated at different corrosive solution.The surface coverage degree θ can be gained by equation (2) [17]:

$$\theta = \frac{CR - CR_i}{CR} \quad (2)$$

The inhibitive effect of HACC for carbon steel is expressed as inhibition efficiency (η_w%) calculated by equation (3)[18-20]:

$$\eta_w\% = \left(\frac{CR - CR_i}{CR}\right) \times 100\% \quad (3)$$

Where CR_i and CR represent average corrosion rates (mmpy) of the tested sheets in corrosive solution containing and without a specified HACC concentration (i), respectively.

2.3. Electrochemical Measurements

The cell equipped with three electrodes was applied to conduct electrochemical experiments. Saturated calomel electrode (SCE) was utilized as the reference electrode. Carbon steel sample with surface area of 1.0 cm^2 and a platinum sheet (2 cm^2, purity 99.9%) (CE) were employed as working electrode and counter electrode, respectively. Potentials of carbon steel were obtained versus SCE and shown in mV. All the experiments were conducted on electrochemical autolab Parstat 2273. In order to reach a steady state and ensure the reliable results, no obvious change should be observed in open circuit potential (OCP), so before electrochemical tests, the system was stabilized for 0.5 h.For potentiodynamic polarization experiments, the potentials vs OCP were obtained from -150 mV to +250 mV. 0.5 mV s^{-1} was used as the scanning rate. EIS test was made at OCPThe frequency varied from 100000 to 0.01 Hz with 10 mV AC amplitude. The experiments were conducted under 30.0±0.1℃controlled by thermostatic water bath in a naturally aerated corrosive solution without stirring.

Cview was employed to analyze the potentiodynamic polarization curves. Nyquist plots were simulated with the suggested model by Zview.

2.4. Surface morphology of carbon steel

Observation of the corrosive morphology of carbon steel was the most visual method to judge the inhibitor performance. The carbon steel specimens were suspended in uninhibited H_2SO_4 solutions and in presence of HACC (100 mg L^{-1}) at 30.0±0.1℃ for 5 h, then taken out, washed and dried. The surface morphologies were obtained using SEM. The size of carbon steel sample was the same to that in weight loss experiments.

3. RESULTS AND DISCUSSION

3.1. Weight loss results

Fig.2 gives corrosion rate and inhibition efficiency after immersion for 5 h at various temperatures. With the gradual rise of HACC concentration, the corrosion rates are prominently reduced while the corrosion inhibition efficiency is enhanced from 10 to 100 mg L^{-1} at the same temperature, which reflects HACC exhibits the inhibition on steel corrosion at the chosen HACC

concentrations under certain temperature. The maximum η_w% is 89.3% with 100 mg L^{-1} HACC at 30℃. The inhibition phenomenon is ascribed to high surface coverage of adsorbed HACC molecules. Before saturation, high concentration and large coverage result in good inhibition performance.. Therefore the corrosion degree of carbon steel surface is decreased drastically [21, 22].

The variations of *CR* and η_w% with temperature are also presented in Fig.2. The reduction in η_w% and an increase in *CR* from 30.0-60℃at specific concentration are observed. The results indicate that η_w% reduced by the increment of temperature is due to the rapid dissolution of carbon steel resulting in HACC molecules detached from steel surface. High temperature causes detachment of more HACC molecules and lower η_w%. But HACC still exhibits inhibitive effect even at the highest temperature (60℃). This phenomenon implies that the stable protective layer formed and protects carbon steel from acid corrosion.

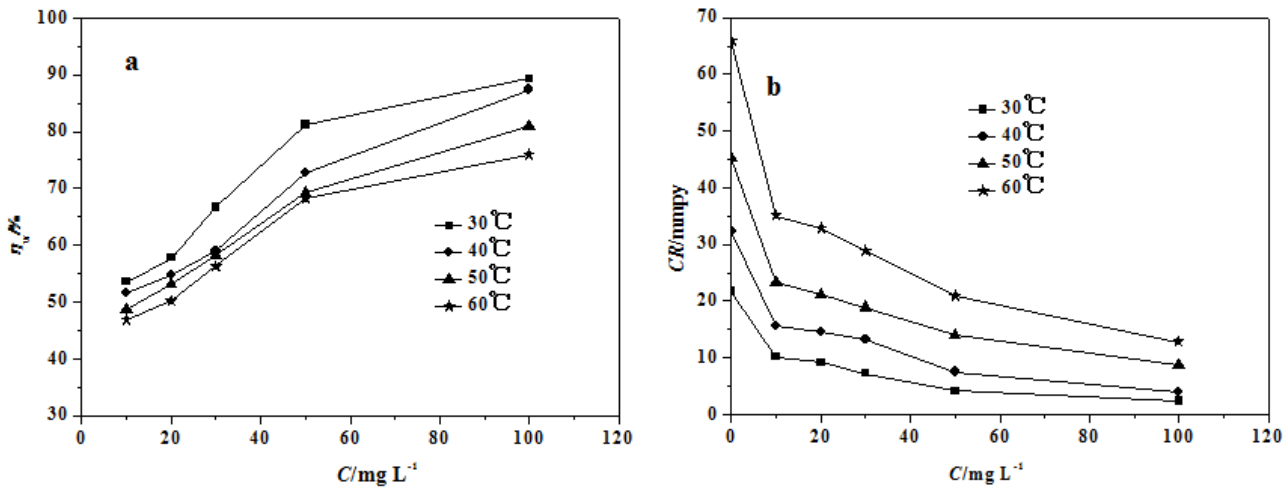

Figure 2. Plots of inhibition efficiency (η_w%) (a) and corrosion rate (*CR*) (b) for carbon steel in uninhibited and inhibited 0.25 M H_2SO_4 solutions at 30-60℃.

3.2. Potentiodynamic polarization curves

The potentiodynamic polarization e measurements may be employed to acquire the kinetic parameters of corrosion reactions of metal. The influence of HACC concentration on potential-current feature was presented in Fig. 3. From Fig.3, the existence of HACC shifts both anodic and cathodic curves towards low current densities even at the smallest concentration. The cathodic and anodic processes are greatly suppressed by HACC compared to those in the blank 0.25 M H_2SO_4 solution. The increase of HACC dosage strengthens this suppression effect.

The retardation of inhibitor for metal corrosion is a dynamic and competitive adsorption/desorption process on the metal surface. It exhibits inhibition effect if the adsorption rate exceeds desorption rate, or it has little inhibition effect on the metal corrosion even accelerates the corrosion. After HACC is added, the cathodic polarization branches show rise to parallel lines and the cathodic current density goes down drastically along with the increased HACC dosage, indicating the mechanism of cathodic reaction is not transformed by HACC and charge transfer leads to the decrease

of the number of H^+ cation on steel surface. HACC adsorption on steel surface downsizes surface area used for cathodic hydrogen reduction reaction.

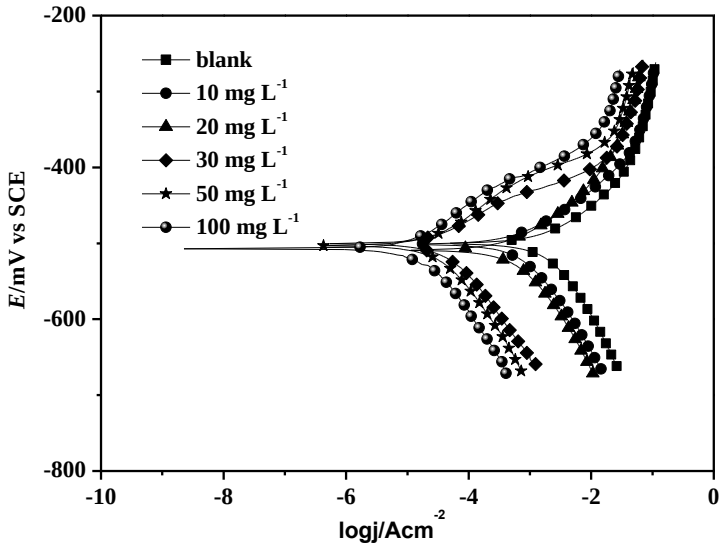

Figure 3. Anodic and cathodic curves of carbon steel electrode in 0.25 M H_2SO_4 solution without and with HACC at 30℃.

For anodic polarization branch, taking 100 mg L^{-1} as an example, at the low over potentials, with the potential increasing, the current density decreases slowly, which indicates that HACC adsorptive film has formed on steel surface [23-24]. At this time, the adsorption rate is over desorption rate. However, the inhibition is weakened with the continuous increase of over potential, even lost. In Fig.3, the current density increases rapidly and the inhibitor exhibits weak inhibition effect on carbon steel reaction as the potential continue to increase positively and reaches to above -400 mV, the potential is called as desorption potential indicating the desorption rate dominates the polarization process.

When the potential exceeds -340 mV the polarization curves exhibits the similar shape to that of the blank solution. Over potential reaches certain value the polarization curve coincides with that of blank solution. This suggests the electrode potential affects inhibition performance greatly. The behavior at higher over potentials is due to the fact that carbon steel dissolved significantly causing desorption of HACC molecules from steel surface [25]. This behavior is not clearly observed at low concentration.

The corresponding electrochemical data extrapolated by polarization plots are presented in Table 1, such as j_{corr}, current density; E_{corr}, corrosion potential; β_c and β_a, cathodic and anodic Tafel slope; η_j%, inhibition efficiency calculated by j_{corr} employing equation(4) [26-27]:

$$\eta_j\,\% = \left(1 - \frac{j_{corr.,i}}{j_{corr.,0}}\right) \times 100\% \qquad (4)$$

Where $j_{corr.,i}$(mA cm^{-2}) and $j_{corr.,0}$ (mA cm^{-2}) are the corrosion current densities in presence of a particular HACC concentration and in blank solution.

Table 1 show in the presence of the HACC, the current density is reduced from 3.2 to 0.019 mA cm^{-2} in accordance with the HACC concentration from 10 to 100 mg L^{-1}, while η_j% improves with the added HACC dosage, the highest value of η_j% is 99.4% at 100 mg L^{-1}. Moreover, the addition of HACC does not shift E_{corr} value to positive direction or negative direction obviously. This indicates that HACC may be defined as a mixed inhibitor, decreasing anodic rate together with cathodic rate simultaneously [28-29]. It was reported that [6, 30], the type of a compound as inhibitor depends on the E_{corr} of metal in contrast to uninhibited solution. The compound is a cathodic or anodic inhibitor when E_{corr} value in inhibited solution is lower or higher 85 mV than that in blank solution. Considering this work, the maximum variation in E_{corr} versus blank solution is 7 mV, indicating that HACC behaves as a mixed inhibitor. Some researchers also reported the similar experimental results [6, 31].

Table 1. Electrochemical kinetic parameters obtained by extrapolation of potentiodynamic polarization curves at 30℃.

Conc. /mg L^{-1}	E_{corr} /mV vs SCE	j_{corr} /mA cm^{-2}	β_a /mV dec^{-1}	β_c /mV dec^{-1}	η_j /%
blank	-501	3.2	102	126	-
10	-496	0.91	80	140	71.6
20	-495	0.83	73	132	74.1
30	-501	0.030	46	94	99.1
50	-508	0.023	48	97	99.3
100	-502	0.019	52	99	99.4

3.3. Electrochemical impedance spectroscopy (EIS)

Fig. 4 recorded Nyquist diagrams of carbon steel at 30℃. The Nyquist plots show single depressed semicircle deviated from ideal semicircle. The phenomenon is due to the frequency dispersion in consistent with the high inhomogeneities of steel surface [32]. The characteristic of Nyquist plots implies that dissolution reaction of carbon steel may be controlled by charge transfer process. Nyquist plots remain the similar appearance to blank solution at chosen concentrations suggesting little variation in mechanism of carbon steel corrosion occurred after addition of HACC [33]. However, their sizes of semicircle increase significantly by increased HACC dosage.. The phenomenon was ascribed to the reduction of corrosion reaction by more HACC adsorption on steel surface [19].

An appropriate equivalent circuit could be applied to simulate the corrosive media/metal interface. Inspection of EIS characteristics in this case, equivalent circuit was adopted to model the H_2SO_4/carbon steel interface (Fig.5). R_s represents Helmholtz resistance; R_{ct} denotes the charge transfer resistance to calculate inhibition efficiency; in order to get more accurate results, *CPE* (one constant phase element) is adopted as the displacement of a pure double-layer capacitor [34], which is composed of two parts such as a component Y_0 and a dispersion coefficient n.

The inhibition efficiency (η_R %) was obtained from R_{ct} by the formula (5) [35].

$$\eta_R\% = \frac{R_{ct}^{i} - R_{ct}}{R_{ct}^{i}} \times 100\% \quad (5)$$

where R^{i}_{ct} and R_{ct} represent charge transfer resistances in inhibited electrolyte and in blank solution, respectively.

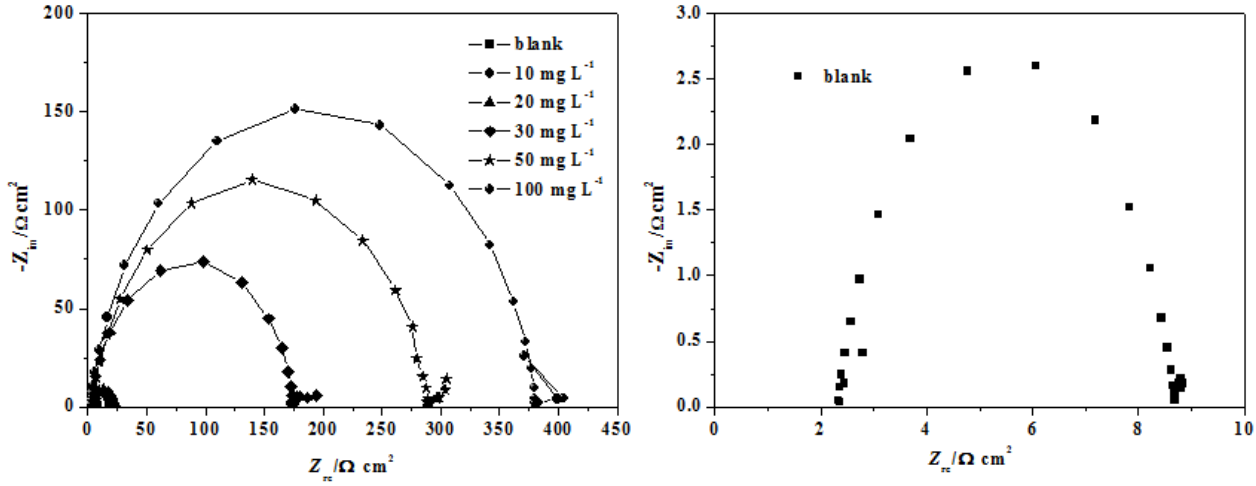

Figure 4. Nyquist plots of carbon steel electrode in 0.25 M H_2SO_4 solution without and with different concentrations of HACC at 30℃.

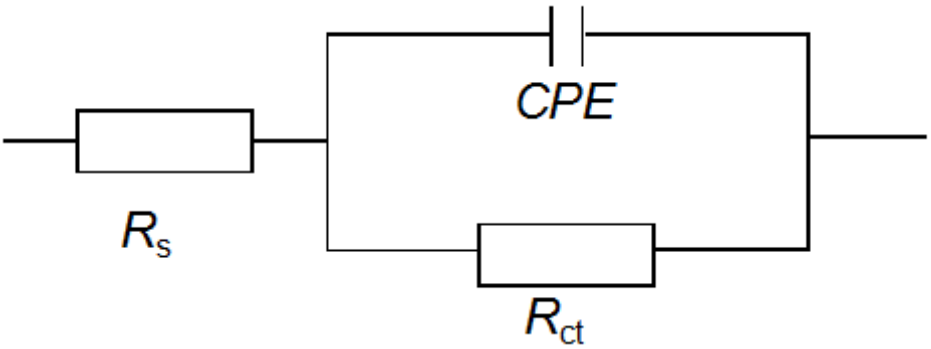

Figure 5. Suggested equivalent circuit model for the studied system.

The fitting results such as R_s, R_{ct}, Y_o, n, η_R% are all tabulated in Table 2. The data suggest presence of HACC leads to the significant increase of charge transfer resistance. R_{ct} enhances with the increasing HACC dosage. The fact indicates charge-transfer process predominantly affects the corrosion impedance. This is due to compact adsorptive film formed at interface [10, 36]. Also, η_R% increases with added amount of HACC which is the consequence of higher surface coverage caused by more HACC molecules adsorbed on steel surface. R_{ct} rises rapidly at low concentration but slowly at high concentration. In comparison with R_{ct}, *CPE* value tends to decrease. The dielectric constant of HACC is lower than water molecules. So the decrease of *CPE* value is due to more adsorbed HACC molecules supplanting H_2O on steel surface [37].It is seen that from the above results of three methods,

the inhibition efficiency is different but gives the same tendency. The value difference in various methods may be due to the different environment conditions and states of carbon steel surface. The difference is unavoidable and acceptable.

Table 2. Impedance parameters and η_R% calculated by R_{ct} for carbon steel electrode in 0.25 M H_2SO_4 solution without and with HACC at 30℃.

Conc. /mg L^{-1}	R_s / Ω cm^2	CPE_{dl}/μF cm^{-2} Y_0 /10^6 S^n Ω^{-1} cm^{-2}	n	R_{ct} / Ω cm^2	η_R /%
blank	2.4	320	0.90	6	
10	1.2	194	0.86	18	66.7
20	2.8	149	0.87	20	70.0
30	2.3	36	0.89	176	96.6
50	2.7	20	0.86	290	97.9
100	2.9	19	0.98	386	98.4

3.4. Adsorption isotherm

Inhibitor molecules interact with carbon steel surface by adsorption. Adsorption isotherm has been extensively adopted to provide explanation of the mode and degree of adsorption. Adsorption isotherm was expressed as equation of surface coverage degree (θ) vs inhibitor concentration (C). The values of C and θ were plotted to model the different adsorption isotherms [38].The obtained weight loss results (equation (2)) for HACC are introduced into various adsorption equations to verify the correlation. The best correlations between θ and C fit the Langmuir adsorption isotherm equation [39]:

$$\frac{C}{\theta} = \frac{1}{K_{ads}} + C \qquad (6)$$

where C represents HACC concentration (mg L^{-1}), θ represents surface coverage derived from inhibition efficiency by weight loss measurements (θ value is equal to inhibition efficiency expressed in decimal form), K_{ads} represents the standard equilibrium constant (L g^{-1}). K_{ads} is used to calculate ΔG^o_{ads} value employing equation(7) [40]:

$$\Delta G^o_{ads} = -RT\ln(1000K_{ads}) \qquad (7)$$

where 1000 g L^{-1} is the concentration of water in solution, R (8.314 J mol^{-1} K^{-1}) is the gas constant, T (K) is absolute temperature, and ΔG^o_{ads} (kJ mol^{-1}) is standard adsorption free energy. C/θ vs C were plotted and shown in Fig. 6, the fitted results such as slope, linear correlation coefficient and the calculated ΔG^o_{ads} and K_{ads} were depicted in Table 3. From equation (6), it can be drawn that the slope of C/θ vs C should be 1. From Table 3, both regression coefficients and slopes are near one clearly denoting that HACC adsorption processes are fit for the Langmuir isotherm at different temperatures. ΔG^o_{ads} values are high and negative suggesting the spontaneous adsorption process of

the HACC molecules [41-43]. In general, ΔG^{o}_{ads} value higher than −20 kJ mol^{-1} is physisorption (inhibitor molecules were adsorbed by coulombic forces). While chemisorption is associated with the value of ΔG^{o}_{ads} lower than −40 kJ mol^{-1}. Chemisorption is the result of electrons sharing or transference between organic molecules and empty d-orbital of the steel [44-45]. ΔG^{o}_{ads} value ranges from −40 to −20 kJ mol^{-1} reflecting a mixed chemisorption and physisorption [46]. The calculated ΔG^{o}_{ads} at different temperatures are in the range (-28.5 to -31.2 kJ mol^{-1}) indicating HACC adsorptions are a mixed process of chemisorption and physisorption.

Table 3. Thermodynamic parameters for HACC adsorption on carbon steel at different temperatures (30-60℃).

Temp. /℃	K_{ads} /L g^{-1}	$-\Delta G^{o}_{ads}$ /kJ mol^{-1}	slope	r Correlation coefficient
30	81.33	28.5	1.00167	0.9932
40	65.04	28.8	1.01428	0.9805
50	69.03	29.9	1.11058	0.9897
60	70.93	31.2	1.18501	0.9926

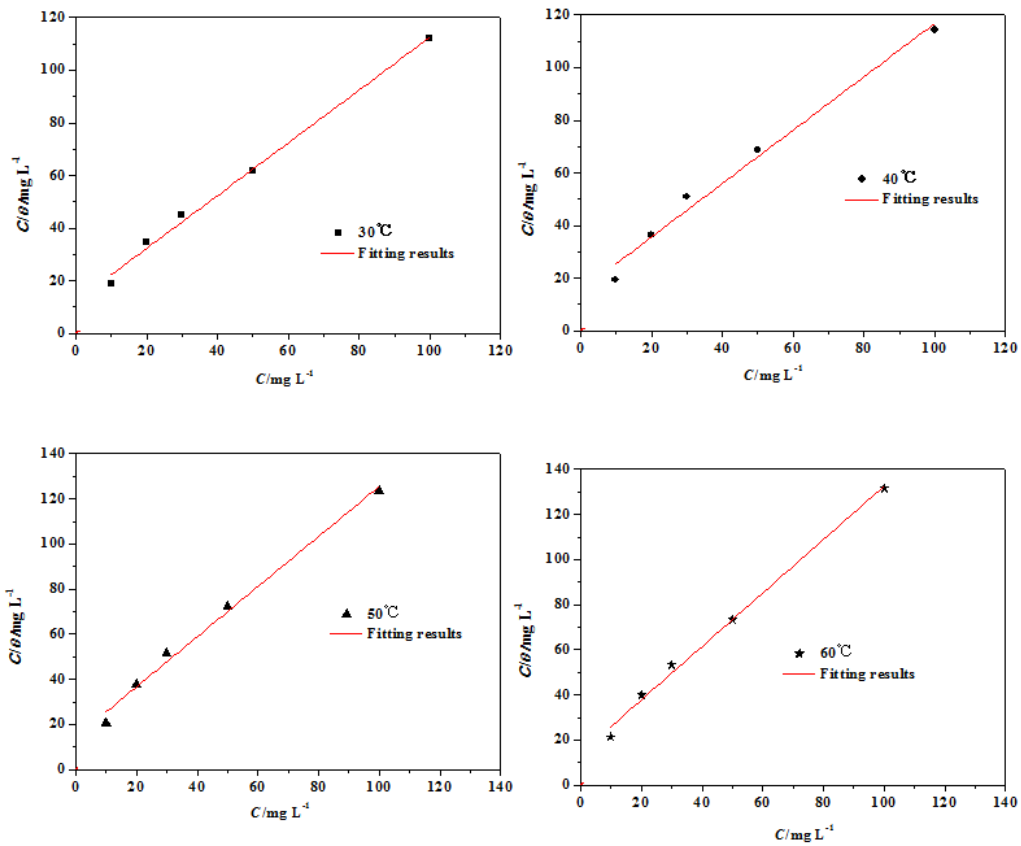

Figure 6. Langmuir's adsorption plots for carbon steel in 0.25 M H_2SO_4 solution containing various concentrations of HACC at different temperatures (30-60℃).

Weight loss and electrochemical results confirmed that HACC exhibited good inhibition effect by adsorption on carbon steel surface. In general, several contributors affect inhibitor adsorption mechanism, such as metal nature, steric configuration of inhibitor molecules, molecular size, electron density of heteroatom, medium type, ect [47-48].

It is well-known that HACC is considered as N-quaternary ammonium salt. In aqueous solution, N-quaternary ammonium salt can be ionized into two parts, one is N-quaternary ammonium cation and the other is inorganic anion. In studied electrolyte, HACC is ionized into HAC^+ and Cl^- following the reaction:

$HACC \rightarrow HAC^+ + Cl^-$

The related results showed that carbon steel surface carried positive charges in H_2SO_4 solution [49-50]. HACC molecules and carbon steel surface are carrying positive charges. Hence, according to the theory of repulsion and attraction, cations HAC^+ exhibit weak adsorption ability. Inhibition efficiency of HACC may depend on two adsorption processes. First, the ionized Cl^- anions may be attracted by Fe^{2+} cations and adsorbed at the electrode/solutions interface through columbic interaction. The Cl^- anions accumulation may lead to too much negative charge towards interface benefiting more HAC^+ cations adsorption, and then the HAC^+ cations can approach to the carbon steel surface covered by already adsorbed anions through electrostatic interactions (physical adsorption). During the process, the Cl^- acts as a bridge connected inhibitor and carbon steel promoting formation of inhibitor adsorptive film. Second, HACC adsorption may occur via transferring unshared electrons from HACC to the empty orbital of the Fe atom (chemisorption) [51]. The transference of unpaired electrons strengthens the inhibition effect of HACC for carbon steel. It is also possible that both physisorption and chemisorption are simultaneous processes.*3.6. Activation energy of corrosion process*

The Arrhenius equation is used to explain the influence of variation of temperature on the reaction rate and is given in the equation (8) [52]:

$$\log CR = \log A - \frac{E_a}{2.303RT} \quad (8)$$

where CR is corrosion rate at different temperatures in presence and absence of HACC (CR comes from weight loss method) (mmpy), E_a is apparent activation energy (kJ mol^{-1}), A is pre-exponential factor (mmpy), R is the universal gas constant (8.314 J mol^{-1} K^{-1}), T is absolute temperature (K).

In this study, plots of log CR vs $1/T$ are depicted in Fig. 7. Plots should be straight lines and slopes are expressed as $-E_a/2.303R$. By linear fitting these plots, the slopes and intercepts are obtained. E_a Values are calculated using slopes and A values are obtained via intercepts, E_a, A and r values are recorded in Table 4. It is revealed that all the regression coefficients are around 1, implying Arrhenius equation can be used to illustrate steel corrosion in 0.25 M H_2SO_4 electrolyte. E_a values of carbon steel corrosion with various concentration of HACC are high compared to blank 0.25 M H_2SO_4 solution. The E_a and A values rise with the enhancement in HACC concentration. The high E_a values indicate HACC molecules are adsorbed on steel surface through electrostatic character (physisorption) [53]. From equation (8), the corrosion rate CR is affected by both E_a and A, the lower corrosion rate is as a result of the combination of the lower A and higher E_a. Usually,, the influence of E_a on corrosion rate is

over *A*, the *A* might become the main factor to affect carbon steel corrosion rate if the variation of *A* is extremely bigger than that of E_a implying lower *A* value can lead to lower corrosion rate and better inhibition effect. In this case, both E_a and *A* increase with the rising HACC concentration, whereas *CR* of carbon steel exhibits the opposite trend (Fig. 2 and Fig. 7));hence, it is concluded that the increment of E_a dominates *CR* of carbon steel, the higher E_a value results in the lower *CR* and higher η%.

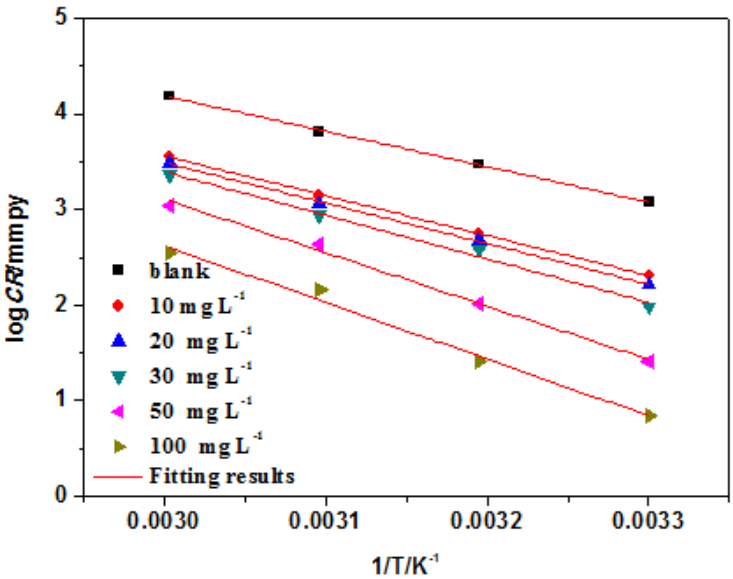

Figure 7. Arrhenius plots for carbon steel in 0.25 M H_2SO_4 solution without and with different concentrations of HACC.**Table 4.** The calculated thermodynamic parameters of adsorption from weight loss measurements.

Conc. /mg L^{-1}	*r* Correlation coefficiency	E_a /kJ mol^{-1}	*A* /mmpy
blank	0.9984	25.6	2.0×10^{15}
10	0.9995	34.7	1.3×10^{16}
20	0.9976	35.3	1.6×10^{16}
30	0.9864	37.9	1.3×10^{17}
50	0.9936	46.5	7.9×10^{19}
100	0.9850	49.3	2.5×10^{20}

3.7. Surface morphology observation

Fig. 8 represents the morphology of carbon steel after immersed in electrolyte for 5 h in presence and absence of 100 mg L^{-1} HACC at 30℃. The photographs reveal that, the surface of the sample taken out from blank solution presents the uniform corrosion with high surface roughness. While carbon steel immersed in inhibited solution is smooth and even with low surface roughness. . The fact is owing to adsorptive barrier of HACC molecules formed on steel surface [36] to separate carbon steel from H_2SO_4 solution. In Fig .8(b), the holes are the defects of carbon steel sample itself not caused by corrosion.

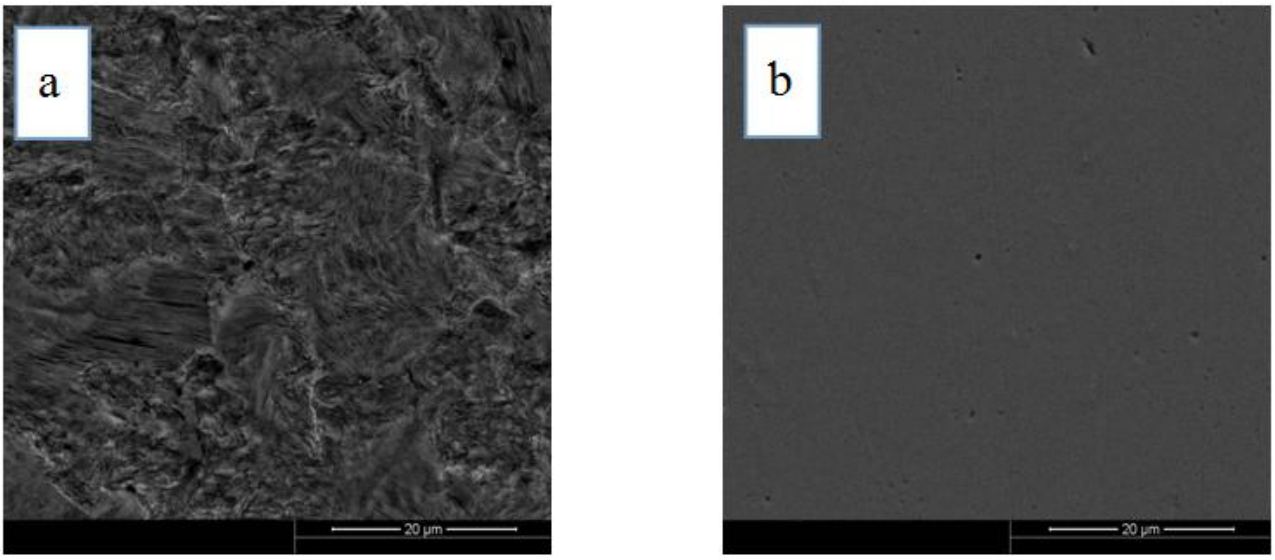

Figure 8. SEM images of carbon steel in 0.25 M H_2SO_4 solution (a) blank; (b) with 100 mg L^{-1} of HACC.

4. CONCLUSION

(1) 2-hydroxypropyltrimethyl ammonium chloride chitosan (HACC) may be used as inhibitor for carbon steel in sulfuric acid medium. HACC shows certain inhibition at all chosen concentration. Inhibition effect increases by increased HACC dosage and decreases with the rise of temperature, the maximum inhibition 89.3% is obtained when 100 mg L^{-1} HACC is added at 30℃, the minimum value reaches 46.9% with 10 mg L^{-1} HACC at 60℃(weight loss measurements). The increment of E_a dominates *CR* of carbon steel. (2) HACC is a mixed inhibitor via retarding hydrogen evolution together with carbon steel oxidation simultaneously. HACC adsorption and desorption is dependent on electrode potential.

(3) EIS plots with single depressed capacitive loop indicate that charge transfer process controlled steel corrosion reaction. Inhibitor HACC enhances R_{ct} while reduces CPE_{dl} in consistence with the displacement of H_2O adsorbed on electrode by HACC molecules.

(4) HACC adsorption follows Langmuir isotherm with a highly spontaneous mixture of physisorption and chemisorption. The mechanism of adsorption is that Cl^- ions act as the bridge connecting carbon steel and HACC molecules.

ACKNOWLEDGEMENT
The authors express grateful acknowledgment to the financial support provided by China Scholarship Council (CSC, Grant No.201408210072) and Ministry of Housing and Urban and Rural Development of the People's Republic of China (Grant No.2014-K4-020).

References

1. A. Adewuyi, A. Göpfertb, T. Wolff, *Ind. Crop. Prod.*, 52 (2014) 439.

2. H. P. Sachin, M. H. Moinuddin Khan, N. S. Bhujangaiah, *Int. J. Electrochem. Sci*., 4 (2009) 134.
3. G. Ji, S. Anjum, S. Sundaram, R. Prakash, *Corros. Sci*., 90 (2015) 107.
4. M. ElBelghiti, Y. Karzazi, A. Dafali, B. Hammouti, F. Bentiss, I. B. Obot, I. Bahadur, E. E. Ebenso, *J. Mol. Liq*., 218 (2016) 281.
5. N. Kıcır, G. Tansug, M. Erbil, T. Tüken, *Corros. Sci*., 105 (2016) 88.
6. A. Hamdy, N.Sh. El-Gendy, *Egypt. J. Petro*., 22 (2013) 17.
7. M. Mobin, S. Zehra, M. Parveen, *J. Mol. Liq*.,216 (2016) 598.
8. M. Finšgar, S. Fassbender, F. Nicolini, I. Milošev, *Corros. Sci*., 51 (2009) 525.
9. H. X. Zhang, D. D. Wang, F. Wang, X. H. Jin, T. R. Yang, Z. Y. Cai, J. Zhang, *Desalination*, 372 (2015) 57.
10. M. Znini, L. Majidi, A. Bouyanzer, J. Paolini, J. M. Desjobert, J. Costb, B. Hammouti, *Arab. J. Chem*., 5(2012) 467.
11. D. K. Singh., S. Kumar, G. Udayabhanu, R. P. John, *J. Mol. Liq*., 216 (2016) 738.
12. S. A. Umoren, M. M. Solomon, U. M. Eduok, I. B. Obot, A. U. Israel, *J. Environ. Chem. Eng*., 2 (2014) 1048.
13. E. A. Noor, *Mater. Chem. Phys*., 131 (2011) 160.
14. N. El Hamdani, R. Fdil, M. Tourabi, C. Jama, F. Bentiss, *Appl. Surf. Sci*., 357 (2015) 1294.
15. A. M. Fekry, R. R. Mohamed, *Electrochim. Acta*., 55 (2010) 1933.
16. M. N. El-Haddad, *Int. J. Biol. Macromol*., 55 (2013) 142.
17. R. A. Prabhu, T. V. Venkatesha, A. V. Shanbhag, G. M. Kulkarni, R. G. Kalkhambkar, *Corros. Sci*., 50 (2008) 3356.
18. C. B. P. Kumar, K. N. Mohana, *Egypt. J. Petro*., 23 (2014) 201.
19. M. A. Hegazy, M. Abdallah, M. K. Awad, M. Rezk. *Corros. Sci*., 81 (2014) 54.
20. M. Scendo, *Corros. Sci.*, 50 (2008) 1584.
21. T. P. Zhao, G. N. Mu, *Corros. Sci*., 41 (1999) 1937.
22. P. Mourya, S. Banerjee, M. M. Singh, *Corros. Sci*., 85 (2014) 352.
23. W. J. Lorenz, F. Mansfeld, *Corros. Sci*., 31 (1986) 467.
24. R. Solmaz, G. Karda, B. Yaz, M. Erbil, *Colloids and Surfaces A: Physicochem. Eng. Aspects*., 312 (2008) 7.
25. B. El Mehdi, B. Mernari, M. Traisnel, F. Bentiss, M. Lagrenee, *Mater. Chem. Phys*., 77 (2002) 489.
26. S. Ghareba, S. Omanovic, *Corros. Sci*., 52 (2010) 2104.
27. N. A. Odewunmi, S. A. Umoren, Z. M. Gasem, *J. Environ. Chem. Eng*., 3 (2015) 286.
28. D. Jayaperumal, *Mater. Chem. Phys*., 119 (2010) 478.
29. W. Li, Q. He, S. Zhang, C. Pei, B. Hou, *J. Appl. Electrochem*., 38 (2008) 289.
30. M. H. Hussin, M. J. Kassim, *Mater. Chem. Phys*., 125 (2011) 461.
31. Q. Hu, Y. B. Qiu, G. A. Zhang, X. P. Guo, *Chin. J.* Chem. *Eng*., 23 (2015) 1408.
32. K. K. Anupama, K. Ramya, K. M. Shainy, A. Joseph, *Mater. Chem. Phys*., 167 (2015) 28.
33. P. B. Raja, A. K. Qureshi, A. A. Rahim, H. Osman, K. Awang, *Corros. Sci*., 69 (2013) 292.
34. J. M. Zhao, H. B. Duan, R. J. Jiang, *Corros. Sci*., 91 (2015) 108.
35. M. Behpour, S. M. Ghoreishi, M. Khayatkashani, N. Soltani, *Mater. Chem. Phys*., 131 (2012) 621.
36. T. Ibrahim, H. Alayan, Y. Al Mowaq, *Prog. Org. Coat*., 75 (2012) 456.
37. M. S. Nooshabadi, M. S. Ghandchi, *J. Ind. Eng. Chem*., 31 (2015) 231.
38. M. M. Saleh, A. A. Atia, *J. Appl. Electrochem*., 36 (2006) 899.
39. J. Saranya, M. Sowmiya, P. Sounthari, K. Parameswari, S.Chitra, K. Senthilkumar, *J. Mol. Liq*., 216 (2016) 42.
40. A. Biswas, S. Pal, G. Udayabhanu, *Appl. Surf. Sci*., 353 (2015) 173.
41. V. R. Saliyan, A. V. Adhikari, *Corros. Sci*., 50 (2008) 55.
42. M. Ozcan, *J. Solid State Electrochem*., 12 (2008) 1653.
43. A. S. Yaro, A. A. Khadom, R. K. Wael, *Alex. Eng. J*., 52 (2013)129.

44. U. M. Eduok, S. A. Umoren, A. P. Udoh, *Arab. J. Chem*., 5 (2012)325.
45. X. Y. Ma, X. H. Jiang, S. W Xia, M. L. Shan, X. Li, L. M. Yu, Q. W. Tang, *Appl. Surf. Sci*., 371 (2016) 248.
46. K. Rose, B. S. Kimd, K. Rajagopal, S. Arumugam, K. Devarayan, *J. Mol. Liq*., 214 (2016) 111.
47. S. Andreani, M. Znini, L. M. Paolini, B. Hammouti, J. Costa, A. Muselli, *Int. J. Electrochem. Sci*., 8 (2013) 11896.
48. A. Singh, Y. H. Lin, E. E. Ebenso, W.Y. Liu, J. Pan, B. Huang. *J. Ind. Eng. Chem*., 24 (2015) 219.
49. A. Popova, M. Christov, A. Vasilev, *Corros. Sci*., 94 (2015) 70.
50. A. Popova, M. Christov, A. Vasilev, A. Zwetanova, *Corros. Sci*., 53 (2011) 679.
51. G. N. Mu, X. M. Li, G. H. Liu, *Corros. Sci*., 47 (2005) 1932.
52. M. Yadav, S. Kumar, T. Purkai, L. O. Olasunkanmi, I. Bahadur, E. E. Ebenso, *J. Mol. Liq*., 213 (2016) 122.
53. M. A. Deyab, *J. Ind. Eng. Chem*., 22 (2015) 384.

© 2016 The Authors. Published by ESG (www.electrochemsci.org). This article is an open access article distributed under the terms and conditions of the Creative Commons Attribution license (http://creativecommons.org/licenses/by/4.0/).